

Optimization of arabica cascara (*Coffea arabica*) ethanolic extract nanoparticle synthesis via ionic gelation using response surface methodology

*Kunarto, B., Larasati, D., Haslina, Rohadi and Azkia, M.N.

Department of Agricultural Product Technology, Universitas Semarang, Semarang 50196, Indonesia

Article history:

Received: 26 September 2024

Received in revised form: 22 December 2024

Accepted: 10 February 2025

Available Online: 19

Novembre 2025

Keywords:

Cascara,
Extract,
Ionic gelation,
Nanoparticles,
Response surface
methodology

DOI:

[https://doi.org/10.26656/fr.2017.9\(6\).222](https://doi.org/10.26656/fr.2017.9(6).222)

Abstract

Cascara, the dried pulp of coffee cherries, shows potential as a source of antioxidants. Nanoparticles derived from the ethanolic extract of Arabica cascara can be synthesized using the ionic gelation method, where chitosan serves as the polycation and sodium tripolyphosphate (STPP) acts as the polyanion. This study aimed to optimize the synthesis of these nanoparticles by crosslinking chitosan with STPP, employing response surface methodology (RSM) with a central composite design (CCD) approach. Arabica cascara extraction was carried out using ultrasonic-assisted extraction at 36°C with 72% ethanol for 31 min, followed by concentration using an evaporator. Nanoparticle synthesis employed the ionic gelation method, varying chitosan (0.05–0.25%) and STPP (0.1–0.4%) concentrations. The resulting nanoparticles were assessed for size, polydispersity index, zeta potential, entrapment efficiency, and antioxidant activity. The results demonstrated that RSM with CCD effectively generated a quadratic model that accurately describes the response variables. The optimal nanoparticle synthesis was achieved with a chitosan concentration of 0.05% and an STPP concentration of 0.36%, producing cascara ethanolic extract nanoparticles with a particle size of 189.30±0.62 nm, a polydispersity index of 0.21±0.01, a zeta potential of 43.33±0.15 mV, an entrapment efficiency of 82.64±0.5%, and an IC₅₀ value of antioxidant activity of 61.71±0.34 ppm. The optimization process determined that nanoparticles of cascara ethanolic extract prepared with 0.05% chitosan and 0.36% STPP achieved excellent homogeneity, stability, and potent antioxidant activity.

1. Introduction

Cascara, the dried skin of the coffee cherry, is a byproduct of coffee processing that includes wet, semi-dry, and dry methods. During wet coffee processing, the byproducts include the outer skin, pulp (39%), mucilage (22%), parchment (39%), and silver skin (Kral *et al.*, 2024). Cascara has shown potential as a source of antioxidants, as phytochemical studies have revealed its content of polyphenols and tannins, including flavan-3-ols, hydroxycinnamic acids, flavanols (Heeger *et al.*, 2017), catechin, rutin, anthocyanidin, ferulic acid (Arpi *et al.*, 2021), hydroxybenzoic acid, caffeic acid, gallic acid, vanillic acid, and coumaric acid (Klingel *et al.*, 2020). Cascara also contains caffeine, chlorogenic acid, and melanoidin (Iriondo-DeHond *et al.*, 2020).

Phenolic compounds, however, are unstable to environmental influences, affecting their bioavailability in the body. One approach to preserving these bioactive

compounds in cascara extract is through nanoencapsulation technology. Nanoparticles formed using polymers can enhance bioavailability and control the release of active substances. The advantages of nanoparticles include improved bioavailability of biomolecules, controlled release of active ingredients, simplified processing, increased stability, enhanced protection against oxidation, and better organoleptic acceptance (Julianawati *et al.*, 2019; Neme *et al.*, 2021). Additionally, nanoparticles can permeate intercellular spaces, as Abdassah (2017) notes, a capability enhanced by their integration with diverse technological approaches.

Nanoparticles can be synthesized through an ionic gelation process. Alehosseini *et al.* (2022) describe this process as the interaction between cations and anions, resulting in the formation of a three-dimensional matrix that encapsulates bioactive compounds within the nanoparticle structure. Chitosan, a biopolymer frequently

*Corresponding author.

Email: bambangkun@usm.ac.id

used in nanoparticle production, offers advantages such as biocompatibility, biodegradability, non-toxicity, and the ability to form a matrix that controls the release of bioactive compounds. Sodium tripolyphosphate (STTP) serves as a crosslinker due to its abundance of negative ions, which enhance particle strength. When STTP is added to a chitosan solution, its polyanions interact with the amino groups of chitosan through electrostatic forces, initiating gel ionization in the chitosan and leading to the formation of nanoparticles (Hoang *et al.*, 2022).

The effectiveness of nanoparticle synthesis via the ionic gelation method depends on achieving a balanced concentration of chitosan, STTP, and the bioactive compound extract (Hoang *et al.*, 2022; Kim *et al.*, 2022). Therefore, optimizing the concentrations of chitosan and STTP is crucial. A common approach to optimization is Response Surface Methodology (RSM). According to Cano-Lamadrid *et al.* (2023), RSM is a mathematical tool widely used to optimize processes by identifying key factorial variables. Nainggolan and Amwar (2023) describe RSM as a technique that combines statistics and mathematics to solve problems related to processes, formulations, or both. Bello *et al.* (2024) further note that the primary purpose of RSM is to enhance the desired response. Within RSM, the Central Composite Design (CCD) is the predominant multivariate optimization approach, combining statistical and mathematical methodologies to explore the effects of various independent variables. This method facilitates the development of empirical models and the design, improvement, and optimization of different procedures (Manzar *et al.*, 2021). Ruiz-Aguilar *et al.* (2023) explain that CCD enables reliable data collection for identifying optimal conditions with a reduced number of experiments. The application of Response Surface Methodology (RSM) with a Central Composite Design (CCD) approach provides an efficient framework for optimizing processes by enabling the identification of significant factors, exploring interactions, and modeling nonlinear relationships with reduced experimental runs. The objective of this research was to optimize the synthesis process of nanoparticles derived from Arabica cascara ethanolic extract using chitosan-STTP crosslinking, employing response surface methodology with a central composite design approach.

2. Materials and methods

2.1 Materials

Arabica cascara was obtained from the Doesoen Sirap coffee education business unit in Semarang Regency. The chemicals used in the study include chitosan (Merck, Germany), sodium tripolyphosphate (STTP) (Merck, Germany), ethanol (Merck, Germany),

Folin-Ciocalteu reagent (Merck, Germany), 2,2-diphenyl-1-picrylhydrazyl (DPPH) (Sigma, USA), and gallic acid (Merck, Germany). The equipment used included grinder (Maksindo, Indonesia), sieve (ASTM Standard, Indonesia), analytical balance (Ohaus PA214, USA), a sonicator bath (3800 Branson, Mexico), a rotary vacuum evaporator (Heidolph, Germany), a spectrophotometer (GENESYS 10S double beam), a particle size analyzer (PSA, Horiba Scientific Nano SZ-100), an FTIR spectrometer (Thermo Nicolet iS10), and glassware (Pyrex).

2.2 Experimental design

In this research, the response surface methodology (RSM) was employed to determine the optimal conditions. The experimental design utilized was a central composite design (CCD), with two factors being varied: chitosan concentration (A) and sodium tripolyphosphate concentration (B) (Table 1). The response variables analyzed included particle size, polydispersity index, zeta potential, entrapment efficiency, and antioxidant activity (RSA-DPPH). The data were processed using Design Expert v. 10.

Table 1. Independent variables and treatment codes.

Independent variables	Code	Range and level		
		-1	0	1
Chitosan concentration (%)	A	0.05	0.10	0.15
STTP concentration (%)	B	0.20	0.30	0.40

2.3 Extract preparation

Cascara Arabica extraction was performed using ultrasonic-assisted extraction at 36°C with a 72% ethanol solvent concentration for 31 min. The extract was concentrated using an evaporator. Nanoparticle synthesis followed the ionic gelation method as described by Soltanzadeh *et al.* (2021). Chitosan concentrations ranged from 0.05% to 0.25%, and STTP concentrations varied from 0.1% to 0.4%. A total of 0.75 grams of cascara ethanolic extract was added to 18 mL of chitosan solution, and the mixture was stirred with a magnetic stirrer at 1500 rpm for 30 min. Then, 3 mL of 0.5% Tween 80 was gradually added drop by drop while stirring at the same speed for 30 min. Afterwards, 9 mL of STTP was added dropwise until a nanoparticle suspension was formed. The cascara ethanolic extract nanoparticles were then evaluated for particle size, polydispersity index, zeta potential, encapsulation efficiency, and antioxidant activity.

2.4 Measurement of nanoparticles, polydisperse index, and zeta potential

Measurement of nanoparticle size, polydispersity index, and zeta potential was conducted following a

modified protocol from Mardiyanto *et al.* (2018). Approximately, 50 μL of the nanoparticle suspension were diluted at a 1:10 ratio. Then, 50 μL of the diluted solution was transferred into a cuvette for analysis using a particle size analyzer (PSA). The PSA instrument emitted monochromatic light, which was detected to determine the particle size, polydispersity index, and zeta potential.

2.5 Entrapment efficiency

The entrapment efficiency was measured using a modified protocol based on the methods described by Kanwal *et al.* (2024) and Supraba *et al.* (2021) with slight modifications. The nanoparticles were centrifuged at 15,000 rpm for 1 h, after which the supernatant was collected. The total phenolic content (TPC) of the supernatant was then measured. The entrapment

$$\text{Entrapment efficiency (\%)} = \frac{(\text{TPC extract} - \text{Supernatant extract})}{\text{TPC extract}} \times 100$$

efficiency was calculated using the following equation:

2.6 Antioxidant activity analysis

Antioxidant activity was conducted following the method of Savić-Gajić *et al.* (2017), with slight modifications. DPPH solution (1 mL) was mixed with 2.5 mL of the sample. After shaking, the mixture was incubated in the dark at room temperature for 30 min. The absorbance was then measured at 517 nm. The percentage of DPPH radical inhibition was calculated

$$\text{DPPH radical inhibition (\%)} = \frac{(A_c - A_s)}{A_c} \times 100$$

using the following formula:

A_c and A_s represent the absorbance of the control and sample, respectively. Antioxidant activity is

expressed as the inhibition concentration (IC_{50}), which indicates the concentration of the sample solution required to inhibit 50% of DPPH free radicals.

3. Results and discussion

The response values for the ethanolic extract nanoparticles of Arabica cascara are presented in Table 2. The model equation, which describes the relationship between chitosan concentration (A) and STPP concentration (B) with the nanoparticle size, polydispersity index, zeta potential, entrapment efficiency, and antioxidant activity, is detailed in Table 3. All responses showed an R^2 value greater than 0.75, indicating a strong correlation between the model predictions and the observed data. The difference between the predicted R^2 and the adjusted R^2 was within 20%, supporting the adequacy of the quadratic model in accurately representing the responses. Moreover, the lack-of-fit value exceeds 0.05, indicating that the responses are not statistically significant (Domingo *et al.*, 2019; Arteaga-Crespo *et al.*, 2020). These findings suggest that the mathematical model provides a reasonable fit for all responses, demonstrating good agreement between the experimental data and the model (Li and Lu, 2016).

3.1 Cascara ethanol extract particle size

The particle size was within the nanoparticle range of 1-1000 nm (Fattahi and Zamani, 2020), specifically between 195.62 and 298.52 nm. The surface response for particle size is illustrated in Figure 1. The interaction between chitosan and STPP concentrations indicates that the smallest particle size was achieved with a chitosan concentration of 0.05% and an STPP concentration of 0.4%.

Table 2. Nanoparticle response values based on central composite design.

Run	Code variable		Actual variable		Response				
	A	B	A Chitosan conc. (%)	B STPP conc. (%)	Particle size (nm)	Polydispersity index	Zeta potential (mV)	Entrapment efficiency (%)	Antioxidant activity IC_{50} (ppm)
1	-1	-1	0.05	0.20	269.11	0.31	37.74	76.96	64.50
2	1	-1	0.15	0.20	298.52	0.34	33.49	73.30	69.37
3	-1	1	0.05	0.40	195.62	0.21	43.94	82.78	60.80
4	1	1	0.15	0.40	225.19	0.30	39.61	79.15	65.30
5	-1.413	0	0.05	0.30	199.28	0.22	43.29	82.57	61.01
6	1.4132	0	0.15	0.30	228.61	0.30	38.93	78.91	65.51
7	0	-1.413	0.10	0.20	269.11	0.35	37.73	76.91	64.67
8	0	1.4132	0.10	0.40	195.73	0.29	43.93	82.78	60.82
9	0	0	0.10	0.30	199.21	0.28	43.29	82.57	60.74
10	0	0	0.10	0.30	199.29	0.29	43.29	82.57	60.71
11	0	0	0.10	0.30	199.22	0.27	43.26	82.55	60.71
12	0	0	0.10	0.30	199.27	0.29	43.27	82.58	60.73
13	0	0	0.10	0.30	199.23	0.29	43.29	82.57	60.71

Table 3. Quadratic equation model of nanoparticle response.

Quadratic response equation	Adjusted R ²	Predicted R ²	p-value	Lack of fit
Particle size = $199.25 + 14.72A - 36.70B + 0.04AB + 14.7A^2 + 33.17B^2$	1	1	<0.0001	0.19
Polydispersity index = $0.28 + 0.3A - 0.3B + 0.01AB - 0.03A^2 + 0.03B^2$	0.95	0.87	<0.0001	0.56
Zeta potential = $43.28 - 2.16A + 3.09B - 0.02AB - 2.15A^2 - 2.43B^2$	1	0.99	<0.0001	0.08
Entrapment efficiency = $82.56 - 1.83A + 2.92B + 0.01AB - 1.81A^2 - 2.71B^2$	1	0.99	<0.0001	0.15
Antioxidant activity (IC ₅₀) = $60.76 + 2.31A - 1.94 - 0.09AB + 2.40A^2 + 1.88B^2$	0.99	0.98	<0.0001	0.54

Note: A is the chitosan concentration; B is the STPP concentration.

As the concentration of chitosan increases, the particle size also increases. These findings align with those reported by Reay *et al.* (2022), who observed that higher chitosan concentrations lead to the agglomeration of chitosan molecules, resulting in larger particle sizes. Conversely, increasing the STPP concentration results in smaller particle sizes. According to Babakhani and Sartaj (2023), STPP acts as a cross-linking agent, and higher STPP concentrations facilitate the formation of cross-linking bonds between the polyanions in STPP and the amino groups in chitosan. This cross-linking effect leads to a reduction in particle size, as the folding structure of

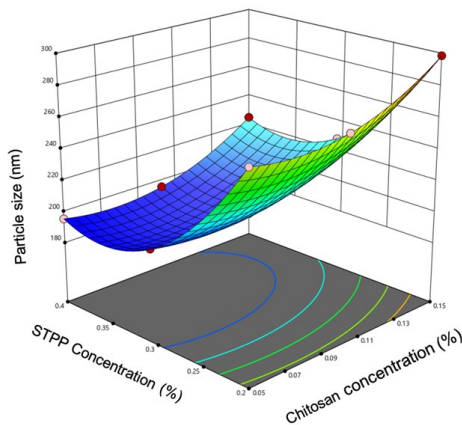


Figure 1. Surface response of particle size.

the dispersed polymer chains becomes progressively smaller.

3.2 Polydispersity index of cascara ethanol extract nanoparticles

The polydispersity index (PDI) values range from 0 to 1, where values close to 0 indicate a higher degree of dispersion homogeneity. A PDI value exceeding 0.5 suggests a lower level of homogeneity (Kadhim and Rajab, 2022). The PDI values for cascara Arabica nanoparticles range from 0.21 to 0.35, indicating relatively homogeneous dispersion, particularly at a chitosan concentration of 0.05% and an STPP concentration range of 0.2-0.4% (Figure 2). The PDI increases with the addition of chitosan, which is associated with particle agglomeration, leading to

settling and clumping in the suspension. This results in a broader particle size distribution and reduced uniformity. Conversely, increasing the STPP concentration results in smaller particle sizes and a lower PDI. The presence of

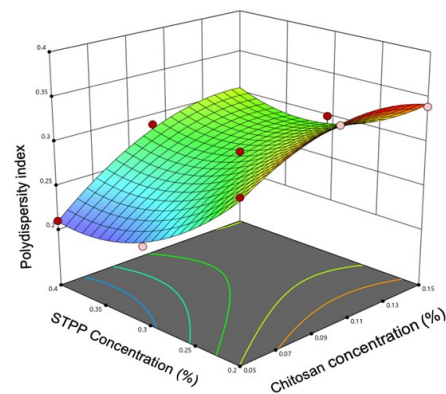


Figure 2. Response surface of polydispersity index.

STPP helps to prevent particle agglomeration during the formation of fine flocs, thereby improving dispersion homogeneity (Wahyuni *et al.*, 2020).

3.3 Zeta potential of cascara ethanol extract nanoparticles

The zeta potential is a key indicator of nanoparticle stability, as it reflects the repulsive forces between particles due to differences in charge. Zeta potential values exceeding +30 mV or falling below -30 mV are indicative of stability, as these values suggest that the electrical charge is sufficient to repel other particles within the nanoparticle system (Kumar *et al.*, 2020). The results showed that the zeta potential decreased with increasing chitosan concentration but increased with increasing STPP concentration. Sawtarie *et al.* (2017) noted that the formation of chitosan-STPP nanoparticles occurs only within specific concentration ranges of chitosan and STPP. In this study, the zeta potential of cascara ethanolic extract nanoparticles was stable, ranging from 33.49 to 43.94 mV, at a chitosan concentration of 0.05% and an STPP concentration of 0.4% (Figure 3). High zeta potential values (greater than ±30 mV) combined with smaller particle sizes enhance Brownian motion, which helps prevent particle settling

and maintains the stability of the dispersion system. The

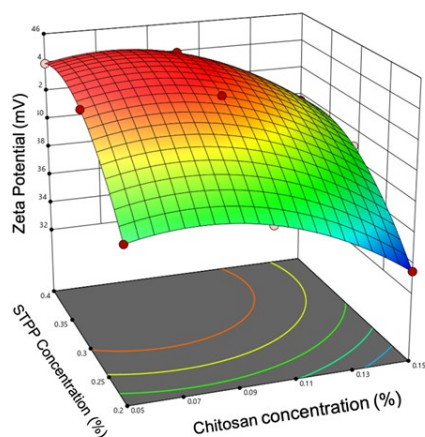


Figure 3. Response surface of zeta potential.

presence of STPP contributes to nanoparticle stability by forming a STPP layer through steric stabilization, which further prevents agglomeration (Arifin *et al.*, 2022; Pratiwi *et al.*, 2019).

3.4 Entrapment efficiency of cascara ethanol extract nanoparticles

The entrapment efficiency is a critical parameter for assessing the effectiveness of the entrapment process. The amount of active compound adsorbed onto nanoparticles is referred to as entrapment efficiency (Pedroso-Santana and Fleitas-Salazar, 2020). The results indicated that the entrapment efficiency of cascara ethanolic extract nanoparticles ranged from 73.30% to 82.78%, with the highest efficiency observed at a chitosan concentration of 0.05% and an STPP concentration between 0.2% and 0.4% (Figure 4). At a chitosan concentration of 0.05%, the entrapment efficiency was higher due to the optimal balance between chitosan and STPP. Increasing the STPP concentration to a certain level enhances cross-linking and improves affinity, resulting in a stronger binding of the extract to the chitosan-STPP matrix, which impedes the rapid release of the extract from the nanoparticles (Kim *et al.*, 2022). In a previous study, the combination of 0.125 mg of chitosan, 0.625 mL of Tween 20, and a stirring speed of 300 rpm yielded the highest entrapment efficiency

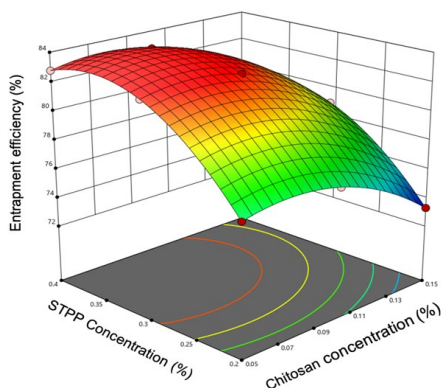


Figure 4. Response surface of entrapment efficiency.

(EE) for the nanoparticles, with a predicted EE value of 84.54% (Alam *et al.*, 2023).

3.5 Antioxidant activity of cascara ethanol extract nanoparticles

The antioxidant activity of the cascara ethanolic extract is robust, with RSA-DPPH (IC_{50}) values ranging from 69.37 to 60.71 ppm. The lowest IC_{50} values were observed at a chitosan concentration of 0.05% and an STPP concentration of 0.4% (Figure 5). Antioxidant activity is correlated with increased entrapment efficiency, which rises with higher STPP concentrations at a chitosan concentration of 0.05%. These findings are consistent with those reported by Solano *et al.* (2023), who observed increased polyphenol content and antioxidant activity following the synthesis of artichoke extract into nanoparticles. Similar results were reported by Kowalczyk *et al.* (2024) for pure thymol extract nanoparticles. This phenomenon is attributed to a reduction in particle size, which increases the surface area of the extract. As a result, the interaction between antioxidant compounds and free radicals is enhanced, leading to a more effective reduction of free radical effects. Alam *et al.* (2023) also studied *Sida cordifolia* hydroalcoholic (SCHA) extract-loaded chitosan nanoparticles (SCHA-CS-NP), which exhibited high antioxidant activity with an IC_{50} value of $86.45 \pm 2.24 \mu\text{g}/\text{mL}$.

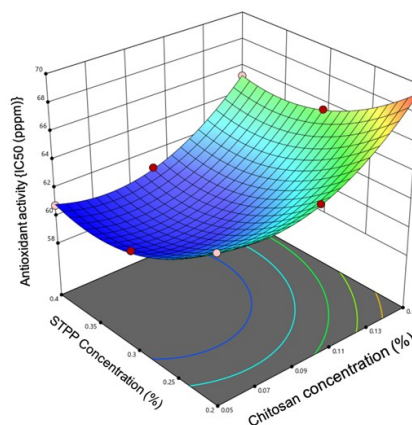


Figure 5. Surface response of antioxidant activity (RSA-DPPH/ IC_{50}).

3.6 Optimization of nanoparticle synthesis

Table 4 presents the criteria used to determine the optimal values. Only values within the specified range were considered. The optimization results indicate that optimal conditions were achieved with a chitosan concentration of 0.05% and an STPP concentration of 0.36%. Under these conditions, the particle size was 189.12 nm, the polydispersity index was 0.21, the zeta potential was 43.27 mV, the entrapment efficiency was 82.35%, and the antioxidant activity (IC_{50}) was 60.42 ppm. The resulting desirability was 0.98, indicating that

the chosen chitosan and STPP concentrations produce a parameter/response value within 98% of the optimal conditions.

Table 4. Criteria for extraction optimization values.

Criteria	Target	Lower limit	Upper limit
Chitosan concentration (A%)	Range	0.05	0.15
STPP concentration (B%)	range	0.2	0.4
Particle size (nm)	Minimize	195.62	298.52
Polydispersity index	Minimize	0.21	0.35
Zeta potential (mV)	Maximize	33.49	43.94
Entrapment efficiency (%)	maximize	73.3	82.78
Antioxidant activity (IC ₅₀ , ppm)	minimize	60.71	69.37

Table 5 displays the predicted response values alongside the actual values obtained under the optimal extraction conditions. The actual response values are as follows: nanoparticle size, 189.30±0.62 nm; polydispersity index, 0.21±0.01; zeta potential, 43.33±0.15 mV; entrapment efficiency, 82.64±0.5%; and RSA-DPPH (IC₅₀), 61.71±0.34 ppm. The residual standard error values ranged from 0.09% to 0.47%, indicating minimal disparity between the actual and predicted response values. According to Sulaiman *et al.* (2017), a residual standard error of less than 5% (0.05) indicates that there is no significant difference between the predicted and actual responses during validation.

3.7 Functional groups of nanoparticles

Based on the Fourier transform infrared (FTIR) spectra (Figure 6), the chitosan spectrum exhibits an O-H functional group at a wave number of 3425.51 cm⁻¹ and an N-H group at 1589.32 cm⁻¹. Interaction between chitosan and the ethanolic extract of Arabica cascara is indicated by a shift in the O-H group wave number from 3425.51 cm⁻¹ to 3429.92 cm⁻¹. Additionally, the N-H absorption shows a shift from 1589.32 cm⁻¹ to 1595.23 cm⁻¹. These shifts are attributed to the interaction between chitosan and the ethanolic extract of Arabica cascara. The FTIR spectrum of cascara Arabica ethanolic extract nanoparticles with STPP reveals a new absorption peak at 1153.43 cm⁻¹, corresponding to the absorption of phosphate groups (P=O), which is likely derived from STPP. The observed shifts in wave number

and intensity in the FTIR results suggest that cross-linking has occurred between the ammonium ions in chitosan, the phosphate ions from STPP, and the ethanolic extract of Arabica cascara. Slavov *et al.* (2024) describe the absorption at 3434 cm⁻¹ for the OH stretching mode in the OH group and the absorption resonance at 3331 cm⁻¹ for the NH₂ group. Rasulu *et al.* (2019) reported that the addition of 0.03% TPP concentration to chitosan coconut crab is evident in the spectrum, which displays specific peaks: the amine group (-NH₂) at 1632 cm⁻¹ and the hydroxyl group (-OH) at 3420 cm⁻¹. The absorption of the amine group (-NH₂) and hydroxyl group (-OH) in chitosan, coconut crab and tripolyphosphate appears at 1650 cm⁻¹ and 3450.32 cm⁻¹, respectively.

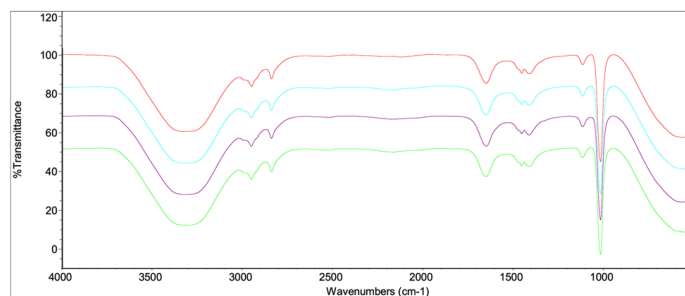


Figure 6. FTIR spectrum of Arabica cascara ethanolic extract nanoparticles. Notes: red (ethanolic extract of Arabica cascara), green (STPP), blue (ethanolic extract of Arabica cascara) and purple (chitosan) color spectra.

4. Conclusion

The application of response surface methodology with a central composite design demonstrates that the quadratic equation model effectively describes the response variables—nanoparticle size, polydispersity index, zeta potential, entrapment efficiency, and antioxidant activity—and accurately aligns with the obtained data for all responses. Optimization results reveal that cascara ethanolic extract nanoparticles formulated with a chitosan concentration of 0.05% and an STPP concentration of 0.36% exhibit high homogeneity, stability, and strong antioxidant activity.

Conflict of interest

The authors declare no conflict of interest.

Table 5. Predicted response values and actual values.

Respond	Predicted response values	Response actual values	Residual standard error (%)
Particle size (nm)	189.12	189.30±0.62	0.09
Polydispersity index	0.21	0.21±0.01	0.32
Zeta potential (mV)	43.27	43.33±0.15	0.13
Entrapment efficiency (%)	82.35	82.64±0.5	0.43
Antioxidant activity (IC ₅₀ ppm)	60.42	61.71±0.34	0.47

Acknowledgements

The author extends gratitude to the Research and Community Service at Universitas Semarang for the financial support of this research. This research was supported by the Internal Competitive Grant Research (PHKI) from the Institute for Research and Community Service at Universitas Semarang, grant number No. 004/USM.H7.LPPM/L/2023.

References

- Abdassah, M. (2017). Nanopartikel dengan Gelasi Ionik. *Farmaka*, 15(1), 45-52. <https://doi.org/10.24198/jf.v15i1.12138.g5643> [In Bahasa Indonesia].
- Alam, P., Imran, M., Ahmed, S., Majid, H. and Akhtar, A. (2023). Chitosan Nanoparticles for Enhanced Delivery of *Sida cordifolia* Extract: Formulation, Optimization and Bioactivity Assessment. *Pharmaceuticals*, 16(11), 1561. <https://doi.org/10.3390/ph16111561>
- Alehosseini, E., Shahiri Tabarestani, H., Kharazmi, M.S. and Jafari, S.M. (2022). Physicochemical, Thermal, and Morphological Properties of Chitosan Nanoparticles Produced by Ionic Gelation. *Foods*, 11(23), 3841. <https://doi.org/10.3390/foods11233841>
- Arifin, M.F., Noviani, Y., Budiati, A. and Hidayanti, I. (2022). Formulasi Nanosuspensi Ekstrak Kering Rimpang Temulawak (*Curcuma xanthorrhiza* Roxb.) dengan Metode Gelasi Ionik dan Uji Aktivitas Antioksidan. *Jurnal Farmamedika*, 7(2), 126-135. <https://doi.org/10.47219/ath.v7i2.163> [In Bahasa Indonesia].
- Arpi, N., Muzaifa, M., Sulaiman, M.I., Andini, R. and Kesuma, S.I. (2021). Chemical Characteristics of Cascara, Coffee Cherry Tea, Made of Various Coffee Pulp Treatments. *IOP Conference Series: Earth and Environmental Science*, 709(1), 012030. <https://doi.org/10.1088/1755-1315/709/1/012030>
- Arteaga-Crespo, Y., Radice, M., Bravo-Sanchez, L.R., García-Quintana, Y. and Scalvenzi, L. (2020). Optimisation of ultrasound-assisted extraction of phenolic antioxidants from *Ilex guayusa* Loes. leaves using response surface methodology. *Heliyon*, 6(1), e03043. <https://doi.org/10.1016/j.heliyon.2019.e03043>
- Babakhani, A. and Sartaj, M. (2023). Optimization of Nickel(II) adsorption by sodium tripolyphosphate crosslinked chitosan using response surface methodology (RSM). *Sustainable Chemistry for the Environment*, 2, 100019. <https://doi.org/10.1016/j.scenv.2023.100019>
- Bello, U., Amran, N.A., Hazwan Ruslan, M.S., Yáñez, E.H., Suparmaniam, U., Adamu, H., Abba, S.I., Tafida, U.I. and Mahmoud, A.A. (2024). Enhancing oxidative stability of biodiesel using fruit peel waste extracts blend: Comparison of predictive modelling via RSM and ANN techniques. *Results in Engineering*, 21, 101853. <https://doi.org/10.1016/j.rineng.2024.101853>
- Cano-Lamadrid, M., Martínez-Zamora, L., Mozafari, L., Bueso, M.C., Kessler, M. and Artés-Hernández, F. (2023). Response Surface Methodology to Optimize the Extraction of Carotenoids from Horticultural By-Products—A Systematic Review. *Foods*, 12(24), 456. <https://doi.org/10.3390/foods12244456>
- Domingo, C.J.A., De Vera, W.M., Pambid, R.C. and Austria, V.C. (2019). Playing with the senses: application of box-behnken design to optimize the bukayo formulation. *Food Research*, 3(6), 833-839. [https://doi.org/10.26656/fr.2017.3\(6\).190](https://doi.org/10.26656/fr.2017.3(6).190)
- Fattahi, F.S. and Zamani, T. (2020). Synthesis of Polylactic Acid Nanoparticles for the Novel Biomedical Applications: A Scientific Perspective. In *Nanochemistry Research*, 5(1), 1-13. Iranian Chemical Society. <https://doi.org/10.22036/NCR.2020.01.001>
- Heeger, A., Kosińska-Cagnazzo, A., Cantergiani, E. and Andlauer, W. (2017). Bioactives of coffee cherry pulp and its utilisation for production of Cascara beverage. *Food Chemistry*, 221, 969-975. <https://doi.org/10.1016/j.foodchem.2016.11.067>
- Hoang, N.H., Le Thanh, T., Sangpueak, R., Treekoon, J., Saengchan, C., Thepbandit, W., Papatthoti, N.K., Kamkaew, A. and Buensanteai, N. (2022). Chitosan Nanoparticles-Based Ionic Gelation Method: A Promising Candidate for Plant Disease Management. *Polymers*, 14(4), 662. <https://doi.org/10.3390/polym14040662>
- Iriondo-DeHond, A., Elizondo, A.S., Iriondo-DeHond, M., Ríos, M.B., Mufari, R., Mendiola, J.A., Ibañez, E. and del-Castillo, M.D. (2020). Assessment of Healthy and Harmful Maillard Reaction Products in a Novel Coffee Cascara Beverage: Melanoidins and Acrylamide. *Foods*, 9(5), 620. <https://doi.org/10.3390/foods9050620>
- Julianawati, T., Hendarto, H. and Widjiati, W. (2019). Penetapan Total Flavonoid, Aktivitas Antioksidan dan Karakterisasi Nanopartikel Ekstrak Etanol Daun Kelor (*Moringa pterygosperma* Gaertn.). *Jurnal Penelitian Kesehatan "SUARA FORIKES"*, 11(1), 49-54. <https://doi.org/10.33846/sf.v11i1.616> [In Bahasa Indonesia].
- Kadhim, Z.J. and Rajab, N.A. (2022). Formulation and Characterization of Glibenclamide Nanoparticles as an Oral Film. *International Journal of Drug Delivery Technology*, 12(1), 387-394. [https://doi.org/10.26656/fr.2017.9\(6\).222](https://doi.org/10.26656/fr.2017.9(6).222)

- doi.org/10.25258/ijddt.12.1.70
- Kanwal, Z., Akhtar, B., Aslam, B. and Arshad, M.I. (2024). Carvone-loaded chitosan nanoparticles alleviate joint destruction by downregulating the expression of pro, inflammatory cytokines and MMP-13 in adjuvant-induced rat model. *Inflammopharmacology*, 33, 269-289. <https://doi.org/10.1007/s10787-024-01618-5>
- Kim, E.S., Baek, Y., Yoo, H.J., Lee, J.S. and Lee, H.G. (2022). Chitosan-Tripolyphosphate Nanoparticles Prepared by Ionic Gelation Improve the Antioxidant Activities of Astaxanthin in the In Vitro and In Vivo Model. *Antioxidants*, 11(3), 479. <https://doi.org/10.3390/antiox11030479>
- Klingel, T., Kremer, J.I., Gottstein, V., de-Rezende, T.R., Schwarz, S. and Lachenmeier, D.W. (2020). A Review of Coffee By-Products Including Leaf, Flower, Cherry, Husk, Silver Skin, and Spent Grounds as Novel Foods within the European Union. *Foods*, 9(5), 665. <https://doi.org/10.3390/foods9050665>
- Kowalczyk, A., Twarowski, B., Fecka, I., Tuberoso, C.I.G. and Jerković, I. (2024). Thymol as a Component of Chitosan Systems—Several New Applications in Medicine: A Comprehensive Review. *Plants*, 13(3), 362. <https://doi.org/10.3390/plants13030362>
- Král, E., Rukov, J.L. and Mendes, A.C. (2024). Coffee Cherry on the Top: Disserting Valorization of Coffee Pulp and Husk. *Food Engineering Reviews*, 16(1), 146-162. <https://doi.org/10.1007/s12393-023-09352-4>
- Kumar, A., Hodnett, B.K., Hudson, S. and Davern, P. (2020). Modification of the zeta potential of montmorillonite to achieve high active pharmaceutical ingredient nanoparticle loading and stabilization with optimum dissolution properties. *Colloids and Surfaces B: Biointerfaces*, 193, 111120. <https://doi.org/10.1016/j.colsurfb.2020.111120>
- Li, P.H. and Lu, W.C. (2016). Effects of storage conditions on the physical stability of *d*-limonene nanoemulsion. *Food Hydrocolloids*, 53, 218-224. <https://doi.org/10.1016/j.foodhyd.2015.01.031>
- Manzar, M.S., Khan, G., Lins, P.V.D., Zubair, M., Khan, S.U., Selvasembian, R., Meili, L., Blaisi, N.I., Nawaz, M., Abdul Aziz, H. and Kayed, T.S. (2021). RSM-CCD optimization approach for the adsorptive removal of *Eriochrome Black T* from aqueous system using steel slag-based adsorbent: Characterization, Isotherm, Kinetic modeling and thermodynamic analysis. *Journal of Molecular Liquids*, 339, 116714. <https://doi.org/10.1016/j.molliq.2021.116714>
- Mardiyanto, M., Fithri, N.A. and Raefy, W. (2018). Optimasi Formula Submikro Partikel Poly (Lactic-co-Glycolic Acid) Pembawa Betametason Valerat dengan Variasi Konsentrasi Poly (Vinyl Alcohol) dan Waktu Sonikasi. *Jurnal Sains Farmasi and Klinis*, 5(1), 55-65. <https://doi.org/10.25077/jsfk.5.1.55-65.2018> [In Bahasa Indonesia].
- Nainggolan, E.A. and Amwar, D. (2023). Optimasi Kondisi Blansir terhadap Whiteness Index Tepung Umbi Kayu menggunakan Response Surface Methodology (RSM). *Fruitset Sains*, 10(6), 418-425. <https://doi.org/10.35335/fruitset.v10i6.3344> [In Bahasa Indonesia].
- Neme, K., Nafady, A., Uddin, S. and Tola, Y.B. (2021). Application of nanotechnology in agriculture, postharvest loss reduction and food processing: food security implication and challenges. *Heliyon*, 7(12), e08539. <https://doi.org/10.1016/j.heliyon.2021.e08539>
- Pedroso-Santana, S. and Fleitas-Salazar, N. (2020). Ionotropic gelation method in the synthesis of nanoparticles/microparticles for biomedical purposes. *Polymer International*, 69(5), 443-447. <https://doi.org/10.1002/pi.5970>
- Pratiwi, G., Martien, R. and Murwanti, R. (2019). Chitosan Nanoparticle as a Delivery System for Polyphenols from Meniran Extract (*Phyllanthus niruri* L.): Formulation, Optimization, and Immunomodulatory Activity. *International Journal of Applied Pharmaceutics*, 11(2), 50-58. <https://doi.org/10.22159/ijap.2019v11i2.29999>
- Rasulu, H., Praseptianga, D., Joni, I.M. and Ramelan, A.H. (2019). Preparation and Characterization of Biopolymer Chitosan Nanofiber from Coconut Crab Shell. *International Journal on Advanced Science, Engineering and Information Technology*, 9(3), 866-873. <https://doi.org/10.18517/ijaseit.9.3.8380>
- Reay, S.L., Jackson, E.L., Ferreira, A.M., Hilken, C.M.U. and Novakovic, K. (2022). Evaluation of The Biodegradability of Chitosan-Genipin Hydrogels. *Materials Advances*, 3(21), 7946-7959. <https://doi.org/10.1039/D2MA00536K>
- Ruiz-Aguilar, G.M.L., Martínez-Martínez, J.H., Costilla-Salazar, R. and Camarena-Martínez, S. (2023). Using Central Composite Design to Improve Methane Production from Anaerobic Digestion of Tomato Plant Waste. *Energies*, 16(14), 5412. <https://doi.org/10.3390/en16145412>
- Savić-Gajić, I., Savić, I., Nikolić, V., Nikolić, L., Popsavin, M. and Rakić, S. (2017). The improvement of photostability and antioxidant activity of trans-resveratrol by cyclodextrins. *Advanced Technologies*, 6(2), 18-25. <https://doi.org/10.25258/ijddt.12.1.70>

doi.org/10.5937/savteh1702018S

- Sawtarie, N., Cai, Y. and Lapitsky, Y. (2017). Preparation of chitosan/tripolyphosphate nanoparticles with highly tunable size and low polydispersity. *Colloids and Surfaces B: Biointerfaces*, 157, 110-117. <https://doi.org/10.1016/j.colsurfb.2017.05.055>
- Slavov, D., Tomaszewska, E., Grobelny, J., Drenchev, N., Karashanova, D., Peshev, Z. and Bliznakova, I. (2024). FTIR spectroscopy revealed nonplanar conformers, chain order, and packaging density in diOctadecylamine- and octadecylamine-passivated gold nanoparticles. *Journal of Molecular Structure*, 1314, 138827. <https://doi.org/10.1016/j.molstruc.2024.138827>
- Solano, M.A.Q., Valenzuela, J.A.P., Silva, C.R.E., Lapa, B.F.C., Cruz, A.R.H., Cervantes, G.M.M. and Flores, D.D.C. (2023). Nanoencapsulation by ionic gelation of polyphenols from artichoke (*Cynara scolymus* L.) residues using ultrasound. *Acta Scientiarum Polonorum Technologia Alimentaria*, 22 (1), 57-69. <https://doi.org/10.17306/J.AFS.2023.1047>
- Soltanzadeh, M., Peighambaroust, S.H., Ghanbarzadeh, B., Mohammadi, M. and Lorenzo, J.M. (2021). Chitosan Nanoparticles as a Promising Nanomaterial for Encapsulation of Pomegranate (*Punica granatum* L.) Peel Extract as a Natural Source of Antioxidants. *Nanomaterials*, 11(6), 1439. <https://doi.org/10.3390/nano11061439>
- Sulaiman, I.S.C., Basri, M., Masoumi, H.R.F., Chee, W.J., Ashari, S.E. and Ismail, M. (2017). Effects of temperature, time, and solvent ratio on the extraction of phenolic compounds and the anti-radical activity of *Clinacanthus nutans* Lindau leaves by response surface methodology. *Chemistry Central Journal*, 11, 54. <https://doi.org/10.1186/s13065-017-0285-1>
- Supraba, W., Juliantoni, Y. and Ananto, A.D. (2021). The Effect of Stirring Speeds to the Entrapment Efficiency in a Nanoparticles Formulation of Java Plums seed Ethanol Extract (*Syzygium cumini*). *Acta Chimica Asiana*, 4(1), 197-103. <https://doi.org/10.29303/aca.v4i1.50>
- Wahyuni, S., Prasetyo, M.A., Eris, D.D., Priyono and Siswanto. (2020). Sintesis dan uji in vitro penghambatan nanokitosan-Cu terhadap pertumbuhan *Fusarium oxysporum* dan *Colletotrichum capsici*. *E-Journal Menara Perkebunan*, 88(1), 52-60. <https://doi.org/10.22302/iribb.jur.mp.v88i1.367> [In Bahasa Indonesia].